Grenze International Journal of Engineering and Technology, Special issue

Transformer Coupled Dual Input Converter for Motor Driving Application

Sreelakshmi C S[1] and Hridhya Mereena George[2]
[1]M.Tech Scholar, Power Electronics, Toc-H Institute of Science and Technology Arakkunnam
Email: slsuresh123@gmail.com
[2]Assistant Professor, EEE Department, Toc-H Institute of Science Technology
Arakkunnam
Email: hridhyamg.19@gmail.com

Abstract*—A two-stage stand-alone scheme consisting of a transformer coupled dual input converter (TCDIC) followed by a conventional three phase full-bridge inverter used for motor driving applications in the area of farming aiming for rural deployment is proposed in this paper. Here battery is used as the energy storage element. This paper is proposed to address the issues involved with the existing system. Solar photovoltaic (PV)- based standalone systems have evolved as a promising solution to the issue of electrification in areas where the grid is not available. The major challenges that are faced by the existing system are : 1) to extract the maximum PV power from the array; 2) to protect the battery from overcharging and over discharging; 3) to covert dc to ac in order to fed the motor. These objectives were satisfied by employing a minimum of three converter stages. This will leads to reduction in reliability and efficiency of the system. The dedicated converter cannot be utilized properly if the PV power remains unavailable for more than half a day. The use of additional converters will increase the component count. The TCDIC can be used to realize maximum power point tracking and proper battery charge control can be maintained. A suitable control strategy for the proposed TCDIC is devised .Simple and efficient control structure is developed for proper operating mode selection and smooth transition between different possible modes. A three phase inverter feeds the motor which is connected at the load terminal. This paper is focused towards the motor driving application. The operation of the existing scheme is verified by using Mat lab simulation studies.

***Index Terms*— Battery charge control; PV-based stand-alone scheme; transformer coupled dual input converter; three phase inverter; and three phase induction motor.**

I. Introduction

In India over 300 million Indian citizens have no access to electricity, and the majority of the population reside in rural areas [1][2].And now a days electricity is recognized as one of the major factors required for the existence of human life. Several initiatives were taken to improve this scenario. Majority of them were based on renewable energy resources. Over the years, the solar photovoltaic (PV) has evolved as one of the promising candidates amongst available renewable energy sources and it is being treated as a bright candidate for electrification in the rural areas where electricity grid is not available. However, the power obtained from the solar PV array is not in a form so that it can be directly delivered to the household or

Grenze ID: 01.GIJET.3.2.1

farming applications. It needs a power electronic interface to convert and control the power output.. Such schemes, commonly termed as standalone schemes, also a battery is used as the energy storage element [3] [4]. The PV array and the battery power output is in dc form. The load is fed by an inverter. The inverters are required to maintain about 350V or more to generate an ac voltage of 230V. A complex maximum power point tracking (MPPT) algorithm [5][6] and additional converters [7]-[10] are required to address the issues involved when subjected to non-uniform insolation levels. The serially connected PV modules or batteries causes considerable reduction in power. The serially connected 12V batteries leads to an increase in the cost of the system. To address the issues mentioned above, a standalone system generally designed with low voltage levels for PV array and the battery in the range of 24-36V. This requires high voltage gain to ensure 230V ac supply at the load terminal which is achieved by employing a low frequency step up transformer at the inverter output. This will increase the size ,weight and volume of the system. To address the above mentioned issue, high gain requirement is provided by using intermediate dc-dc converters. It includes about three converter stages. This will leads to poor efficiency and makes the system less reliable. In [14]-[17], a dedicated converter is used to realize MPP operation. But if, PV power remains unavailable for half a day, the proper utilization of converter will not be possible. A paper is presented in [18]- [20], where the use of dedicated converters are avoided. To address the limitations associated with [18]-[20] a transformer coupled dual input converter (TCDIC) based standalone system [21] is used. By connecting PV array in series with the battery enables the boosting capability of the converter. TCDIC can be used to perform MPPT operations, battery over charge and over discharge control and voltage boosting by employing a proper algorithm. DC-AC conversion is employed by using a standard three phase full bridge inverter. Electricity is not only used for house hold and lighting purposes, but also it allows for mechanization of many farming operations. Farming plays an important role in the area of rural deployment. This paper proposes a suitable and efficient method for watering applications for the purpose of farming. This paper is proposed as an application of [21]. The output of the 3phase inverter is used to drive a three phase induction motor, which can be used to water the crops even after daylight hours. And thus, greater productivity can be achieved at a reduced cost.

The basic philosophy of this scheme is presented in [20],[21] and [22]. Detailed simulation is included in this paper. The operating principle of TCDIC is presented in section II. The control strategy for TCDIC is presented in section III. Results of detailed simulation are presented in section IV.

II. Operating Principle of TCDIC

The schematic diagram of the TCDIC is shown in figure 1.The inductor current is assumed to be continuous. The switches S1 and S2 are operated in complementary fashion. All semiconductor devices and passive elements are assumed to be ideal in the following analysis.

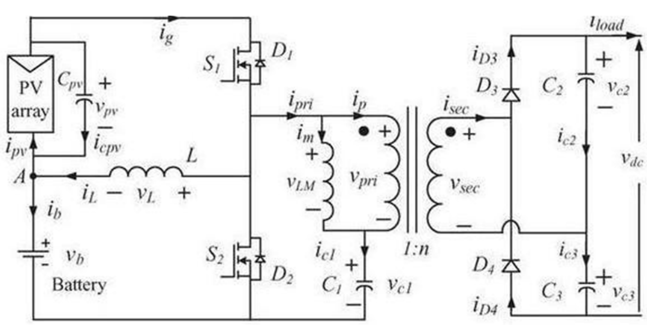

Fig. 1. Schematic circuit diagram of TCDIC

A. Operation of the Converter When Inductor Current is Positive

The waveforms of the currents flowing through and voltages across different key circuit elements of TCDIC, while the current flowing through the inductor L is positive, are shown in Fig. 2(a). The various possible switching modes during this condition are analyzed in this section.

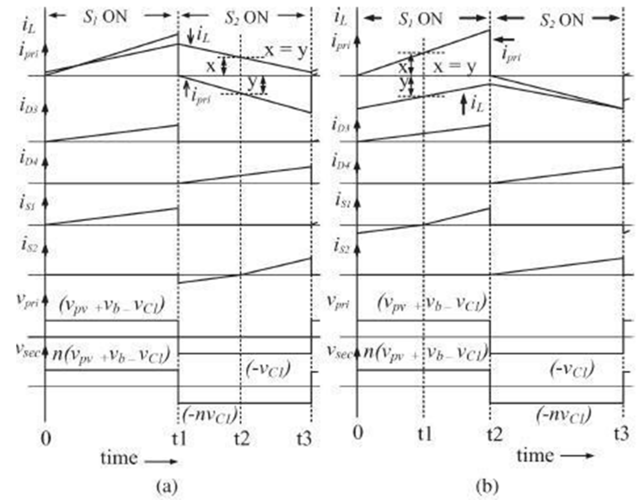

Fig. 2. Waveforms of currents flowing through and voltage across different key circuit elements of TCDIC when (a) i_L is positive and (b) i_L are negative

a) Mode I (0 to t_1; S_1 and D_3 conducting): When S_1 is turned on, the PV array voltage V_{pv} will appear across L, and the inductor current i_L increases. The voltage impressed across the primary winding of the transformer is $V_{pri} = (V_{pv} + V_b - V_{c1})$, where V_b is the battery voltage and V_{c1} is the voltage across the capacitor C_1. Hence, the primary current of the transformer, i_{pri}, is increased, and the capacitor C_1 is charged. As a result the secondary current of the transformer, i_{sec}, also increases. The diode D_3 is forward biased and the capacitor C_2 is charged. The voltage across C_2 is given by $V_{C2} = n(V_{pv} + V_b - V_{c1})$, where n is the turns ratio of the transformer. The equivalent diagram of TCDIC during this mode is shown in Fig. 3.

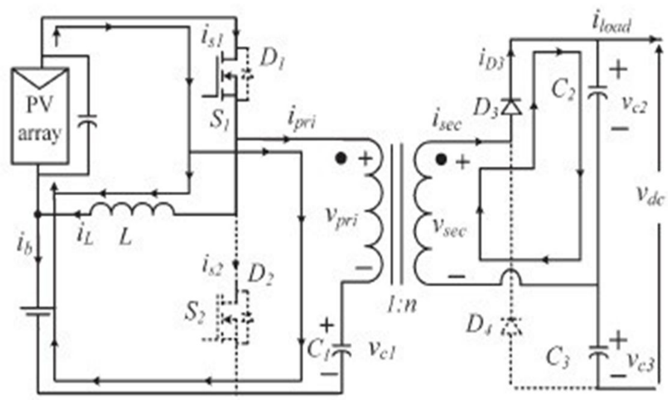

Fig. 3. Equivalent circuit diagram of TCDIC when operating in mode I and inductor current is positive

b) Mode II (t_1 to t_2; D_2 and D_4 conducting): In the beginning of this mode S_1 is turned off and S_2 is turned on. As S_1 is turned off, i_{pri} becomes zero. Since $i_L > i_{pri}$, the diode D_2 starts conducting. The voltage across L is $V_L = V_b$ and hence, i_L starts decreasing. The voltage across the primary winding of the transformer is $V_{pri} = -V_{c1}$, and hence, i_{pri} becomes negative and starts decreasing, thereby discharging C_1. The secondary current of the transformer, i_{sec}, is reversed, and the diode D_4 is turned on. The capacitor C_3 is getting charged, and the voltage across C_3 can be expressed as $V_{C3} = nV_{c1}$. During this mode, $i_L > -i_{pri}$ and diode D_2 is forward biased. This mode continues until i_L becomes equal to $-i_{pri}$. The equivalent circuit diagram of TCDIC during this mode is shown in Fig. 4(a).

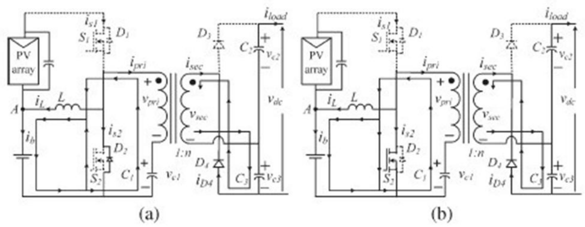

Fig. 4. Equivalent circuit diagram of TCDIC when inductor current is positive: (a) Mode II and (b) mode III

c) Mode III ($t2$ to $t3$; $S2$ and $D4$ conducting): When i_L becomes smaller than i_{pri}, the diode $D2$ is reverse biased, and the switch $S2$ starts conducting. The remaining operation is same as that of mode II. The equivalent circuit diagram of the converter during this mode is shown in Fig. 4(b).

III. Operation of the Converter when Inductor Current is Negative

The waveforms of the currents flowing through and volt- ages across different key circuit elements of TCDIC, while the Current flowing through the inductor L is negative, are shown in Fig. 2(b). The various possible modes are analyzed in this section.

d) Mode I (0 to $t1$; $D1$ and $D3$ conducting): This mode begins when $S1$ is turned on and $S2$ is turned off. At the starting of this mode, i_L is negative, and i_{pri} is zero. Hence, the diode $D1$ starts conducting. The rest of the operation is the same as that of mode I discussed in the previous section. This mode continues until i_{pri} becomes equal to -i_L. The equivalent circuit diagram of TCDIC during this mode is shown in Fig. 5(a).

e) Mode II ($t1$ to $t2$; $S1$ and $D3$conducting): When ipri becomes greater than -i_L, the diode $D1$ is reverse biased, and the switch $S1$ starts conducting. The remaining operation is the same as that of mode I discussed in the previous section. The equivalent circuit diagram of TCDIC during this mode is shown in Fig. 5(b).

III. Operation of the Converter when Inductor Current is Negative

The waveforms of the currents flowing through and volt- ages across different key circuit elements of TCDIC, while the Current flowing through the inductor L is negative, are shown in Fig. 2(b). The various possible modes are analyzed in this section.

d) Mode I (0 to $t1$; $D1$ and $D3$ conducting): This mode begins when $S1$ is turned on and $S2$ is turned off. At the starting of this mode, i_L is negative, and i_{pri} is zero. Hence, the diode $D1$ starts conducting. The rest of the operation is the same as that of mode I discussed in the previous section. This mode continues until i_{pri} becomes equal to -i_L. The equivalent circuit diagram of TCDIC during this mode is shown in Fig. 5(a).

e) Mode II ($t1$ to $t2$; $S1$ and $D3$conducting): When ipri becomes greater than -i_L, the diode $D1$ is reverse biased, and the switch $S1$ starts conducting. The remaining operation is the same as that of mode I discussed in the previous section. The equivalent circuit diagram of TCDIC during this mode is shown in Fig. 5(b).

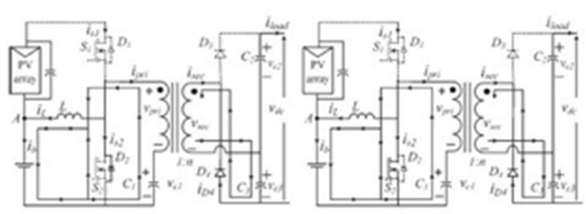

Fig. 5. Equivalent circuit diagram of TCDIC when inductor current is negative: (a) Mode I and (b) mode II

f) Mode III ($t2$ to $t3$; $S2$ and $D4$ conducting): This mode begins when $S1$ is turned off and $S2$ is turned on. In this, both i_L and i_{pri} are negative, and the switch $S2$ conducts. The neg- ative current in the primary winding of the transformer results in negative current in the secondary winding of the transformer. Thus diode

$D4$ is forward biased, and the capacitor $C3$ gets charged. During operation in this mode, $V_L = -V_b$, $V_{pri} = V_{c1}$, and $V_{c3} = nV_{c1}$. The equivalent circuit diagram of TCDIC during this mode is the same as that shown in Fig. 4(b), except that the direction of i_L is reversed.

From Fig.1, the voltage V_L across the inductor L can be expressed as:

$V_L = V_{pv}$ when $S1$ is on.

$V_L = -V_b$, when $S2$ is on.

Thus the average voltage drop across the inductor is

$V_L = DV_{pv} - (1-D)V_b$

where D is the duty ratio of the switch $S1$.The average voltage drop across the inductor is equated to zero.

$$V_{pv} = \frac{(1-D)V_b}{D} \quad (1)$$

By varying D, the PV voltage can be controlled .Thus the MPPT operation of the PV array can be achieved through a proper manipulation of D. The average output voltage of the TCDIC, Vdc, is given by $V_{dc} = (V_{C2} + V_{C3}) = [n(V_b + V_{pv} - V_{C1}) + nV_{C1}] = n(V_b + V_{pv})$. Applying KCL at point A of Fig. 1, $i_L + i_{cpv} = i_b + i_{pv}$. Considering the average values of i_L, i_{cpv} i_b, and i_{pv} over a switching cycle and i_{cp-v} is assumed to be zero. Thus, $I_b = i_L - i_{pv}$. From this, it can be noted that for $i_L > i_{pv}$, the battery is charged and, for $i_L < i_{pv}$, the battery is discharged. Thus, for a given i_{pv}, battery charging and discharging can be controlled by controlling i_L. The details of the control strategy devised for TCDIC are discussed in Section IV.

IV. Control Strategy

The main functions of the controller of the stand-alone scheme are as follows: 1) extraction of maximum power from the PV array; 2) manipulates the battery usage without violating the limits of overcharge and over discharge; and 3) dc-ac conversion. The details of the control algorithm devised for TCDIC are presented in this section.

The PV array voltage V_{pv} and current i_{pv} are given as input to the MPPT algorithm and the maximum PV voltage is generated by the MPPT control block. The V_{mpp}, i_{pv} and Vpvr (a reference voltage) is given to the decision making block, DMB 1. Inside the DMB 1, it will check the condition whether ipv > 0, if it satisfies the condition, then V_{pvref} is generated. Then the mode will be MPPT mode. If $i_{pv} <$ 0 then battery only mode is chosen such that V_{mpp} will be V_{pvr}.Thus generated V_{pvr} is compared with V_{pv} within a PI controller. And i_L star is generated. The upper and lower limits of i_L star is generated to limit the battery over charge and over discharge. This is executed by the decision making block DMB 4 . By trial and error method the overcharging and over discharging battery current limits are obtained and in the next step those conditions are eliminated so as to maintain the charging and discharging level of the battery. When i_{Lref} remains within its prescribed limit, the system operates either in MPPT mode (for $i_{pv} > 0$) or in Battery Only (BO) mode (for i_{pv} 0). The over discharge limit of the battery is reached when i_{Lref} hits its lower limit. DMB-3 withdraws gating pulses from all the switches and shuts down the system. When the battery overcharging limit is attained, i_{Lref} hits its upper limit. This situation arises only when the system is operating in MPPT mode In this condition, i_{Lref} is limited to I_{Lmax} to limit the battery charging current to I_{bmax}. As the battery charging current is limited to I_{bmax}, power consumed by the battery is restricted to P_{bmax}. This makes the available PV power more than (Pl $+P_{bmax}$). This extra PV power starts charging the PV capacitor, and its voltage increases beyond V_{mpp}, thereby shifting the PV operating point toward the right side of the MPP point, and the power extracted from the PV array reduces. This process continues until the power drawn from the PV array becomes equal to (Pl + P_{bmax}). Hence, during operation of the system in non-MPPT mode, the PV array is operated at a point on the right side of its true MPP, and hence, $P_{pv} < P_{mpp}$. If there is a decrement in load demand while operating in non-MPPT mode, power drawn from the PV array becomes more than (Pl + P_{bmax}), and this excess power drawn starts charging the PV capacitor, thereby shifting the operating point of the PV further toward the right side of its previous operating point. In case of an increment in the load demand, the power drawn from the PV array falls short of supplying the load demand and the dc-link capacitors, and the PV capacitor starts discharging. As the voltage of the PV capacitor falls, the operating point of the PV array shifts toward the left side from its previous operating point. This leads to an increment in the power drawn from the PV array, and this process continues until the power balance is restored. In case the load demand increases to an extent such that the PV power available at its MPP falls short to supply this load, the battery will come out of its charging mode, i_{Lref} will become less than I_{Lmax}, and the system operates in MPPT mode.

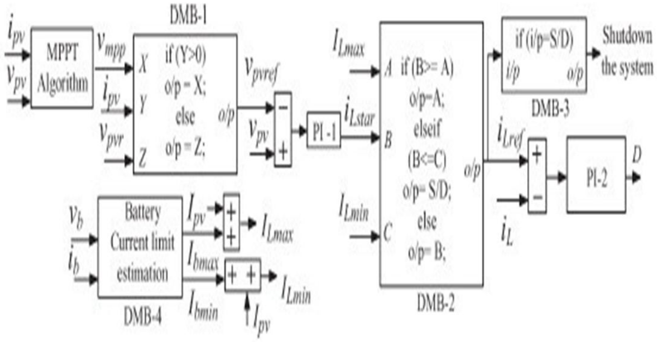

Fig. 6. Control structure for the proposed TCDIC

V. SIMULATED PERFORMANCE

The figure given below shows the parameters used for the existing system.

Parameter	Value
power rating	500 VA
Transformer turns ratio, n	6
Capacitors	C_{pv}=2000 μF, $C_b = 1000\mu$F $C_f = 8\mu$F, $C_1 = 470\mu$F, $C_2 = C_3 = 1000\mu$F
Inductors	L_b=1 mH, L =3 mH, L_f = 2.5 mH
Switching frequency, F_s	15 kHz
MPPT algorithm	Incremental conductance
PI controller gains	For PI-1: K_p=0.068, K_i=.25 For PI-2: K_p=0.03, K_i=1

Fig. 7. Parameters/Elements Used For Stand-Alone System

The system shown in Fig. 8 is simulated on Matlab/Simulink platform, and the simulated responses obtained under different operating conditions are presented in this section.

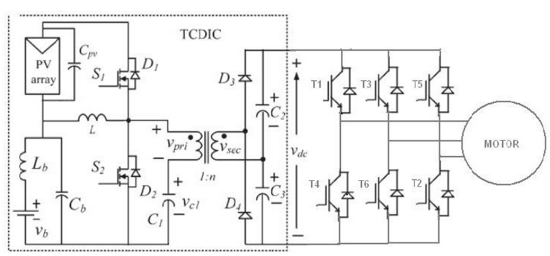

Fig. 8. Schematic of the complete stand-alone scheme

The simulated waveforms are shown below. The first case analyzed is the steady state condition. The Fig.9, Fig.10, Fig.11,Fig.12,Fig.13 shows the waveforms of PV Current i_{pv} , V_{pv} , DC link voltage, the battery current and the pulse generated for the switches in the power circuit respectively.

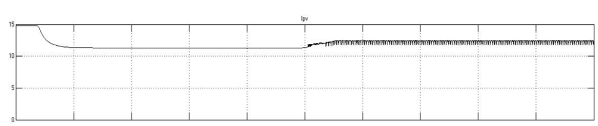

Fig. 9. Simulated response of the system under steady state operation showing PV current, i_{pv}

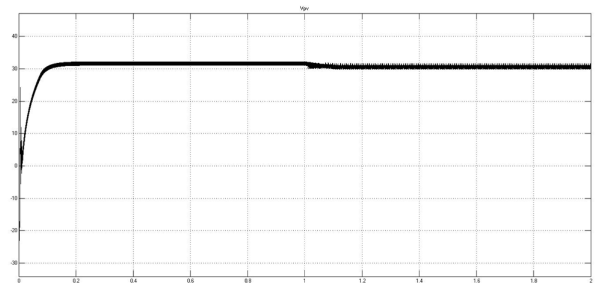

Fig. 10. Simulated response of the system under steady state operation showing PV voltage, V_{pv}

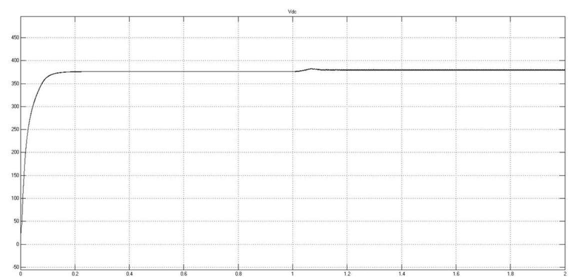

Fig. 11. Simulated response of the system under steady-state operation in MPPT mode showing the dc link voltage V_{dc}

The second case shows the transition between MPPT and non MPPT modes. Here both the load and insolation levels are varied. The simulated waveforms are shown below. The Fig.14, Fig.15, Fig.16,Fig.17 shows the waveforms of PV Current i_{pv} , V_{pv} , DC link voltage ,the battery current and the pulse generated for the switches in the power circuit respectively.
The third case shows the battery only mode. The simulated Waveforms are shown below. The Fig.18, Fig.19, Fig.20, Fig.21,Fig.22 shows the waveforms of PV Current i_{pv} , V_{pv} , DC link voltage, the battery current and the pulse generated for the switches in the power circuit is shown below respectively.

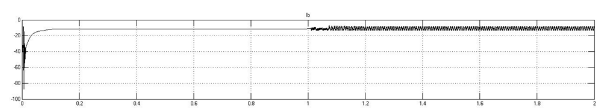

Fig. 12. Simulated response of the system under steady-state operation in MPPT mode showing the battery current I_b

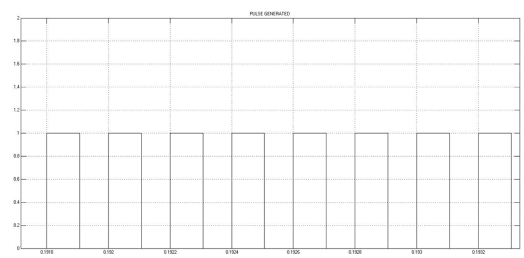

Fig. 13. Pulse generated for the switches in the power circuit

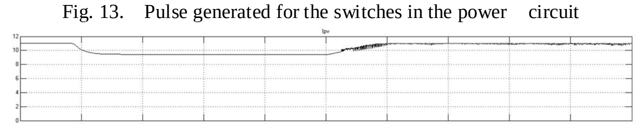

Fig. 14. Simulated response of the system during the transition between MPPT mode and non-MPPT mode showing PV current, i_{pv}

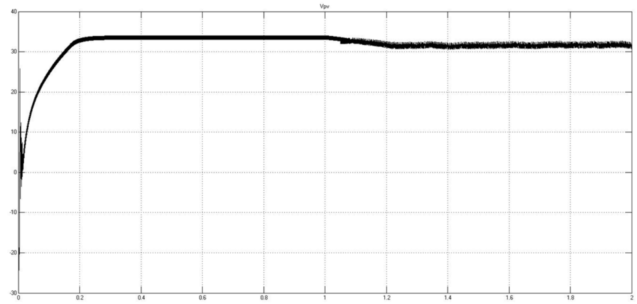

Fig. 15. Simulated response of the system showing PV voltage during the transition between MPPT mode and non-MPPT mode, V_{pv}

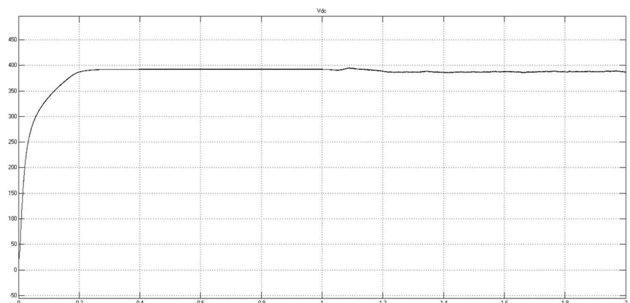

Fig. 16. Simulated response of the system in the transition between MPPT mode and non-MPPT mode showing the dc link voltage V_{dc}

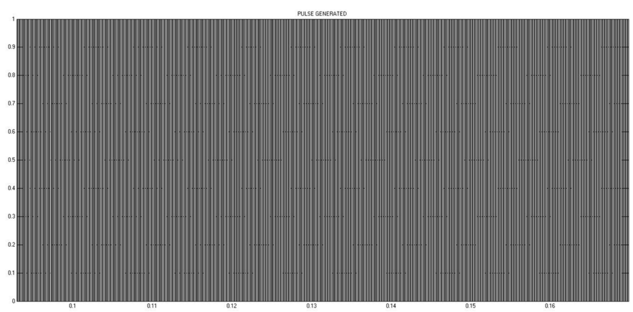

Fig. 17. Pulse generated for the switches in the power circuit during the transition from MPPT mode to non-MPPT m o d e

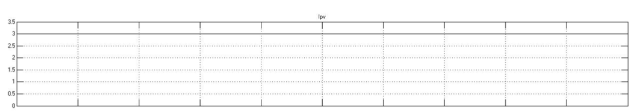

Fig. 18. Simulated response of the system during the battery only mode showing PV current, i_{pv}

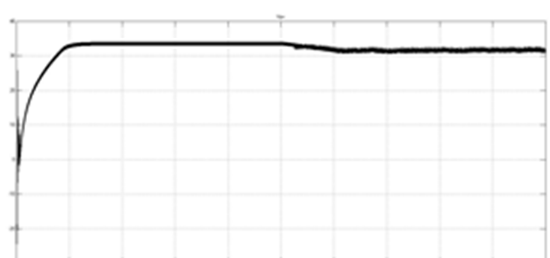

Fig. 19. Simulated response of the system showing PV voltage during the battery only mode, V_{pv}

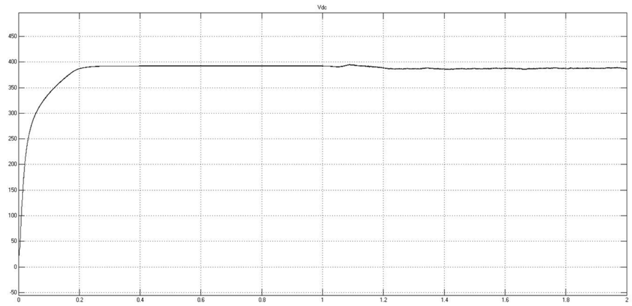

Fig. 20. Simulated response of the system during the battery only mode showing the dc link voltage V_{dc}

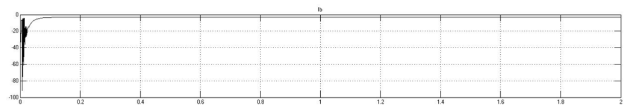

Fig. 21. Simulated response of the system during the during the battery only mode showing the battery current I_b

The load voltage measured across the three phase induction motor for the MPPT mode is shown in Fig.23.

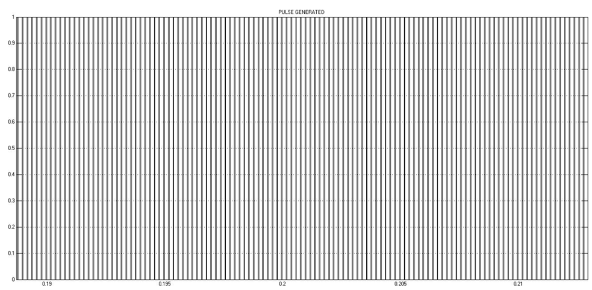

Fig. 22. Pulse generated for the switches in the power circuit during the battery only mode

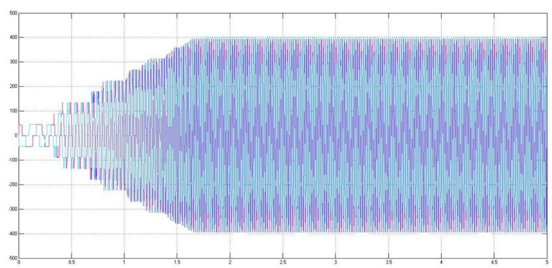

Fig. 23. Simulated response of the load voltage

VI. CONCLUSION

A transformer coupled dual input converter for the motor driving application is proposed in this paper. It is realized by involving an TCDIC followed by a conventional three phase full-bridge dc to ac inverter and a three phase induction motor. The salient features of the converter is as follows 1) The MPPT of the PV array, charge control of the battery, and boosting of the dc voltage are accomplished in a single converter; 2) does not require a dedicated converter for ensuring MPP operation
3) lesser component count as only two power conversion stages are required; 4) simple and efficient control structure ensuring proper operating mode selection and smooth transition between different possible operating modes .The proposed paper can applied in the area of farming. The motor speed and torque are analyzed . The scheme is verified by performing detailed simulation studies.

REFERENCES

[1] Electricity sector in India, Wikipedia, [Accessed: Nov. 3, 2014].[Online].

[2] Access to electricity ” [Accessed: Nov. 3, 2014]. [Online]. Available: http://data.worldbank.org/indicator/EG.ELC.ACCS.ZS

[3] M. Sechilariu, B. Wang, and F. Locment Building integrated photovoltaic system with energy storage and smart grid communication , *IEEE Trans. Ind. Electron.*, vol. 60, no. 4, pp. 16071618, Apr. 2013.

[4] Y. M. Chen, A. Q. Huang, and Y. Xunwei A high step-up three-port dc-dc converter for stand-alone PV/battery power systems , *IEEE Trans.Power Electron*, vol. 28, no. 11, pp. 50495062, Nov. 2013

[5] B. N. Alajmi, K. H. Ahmed, S. J. Finney, and B. W. WilliamsA maximum power point tracking technique for partially shaded photovoltaic systems in microgrids ,*IEEE Trans. Ind. Electron*,vol. 60, no. 4, pp. 15961606, Apr. 2013.

[6] M. Miyatake, M. Veerachary, F. Toriumi, N. Fujii, and H. KoMaximum power point tracking of multiple photovoltaic arrays: A PSO approach , IEEE Trans. Aerosp. Electron. Syst,vol. 47, no. 1, pp. 367380, Jan. 2011.

[7] J. T. Stauth, M. D. Seeman, and K.KesarwaniResonant switched capacitor converters for sub-module distributed photovoltaic power management , *IEEE Trans. Power Electron.*,vol. 28, no. 3, pp. 11891198, Mar. 2013.

[8] T. Shimizu, M. Hirakata, T. Kamezawa, and H.Watanabe Generation con- trol circuit for photovoltaic modules , *IEEE Trans. Power Electron,*,vol. 16, no. 3, pp. 293300, May 2001.

[9] H. J. Bergveld et al.,Module-level dc/dc conversion for photovoltaic sys- tems: The delta-conversion concept , *IEEE Trans. Power Electron.,*,vol. 28, no. 4, pp. 20052013, Apr. 2013.

[10] P. S. Shenoy, K. A. Kim, B. B. Johnson, and P. T. Krein,Differential power processing for increased energy production and reliability of photovoltaic systems, ,*IEEE Trans. Power Electron*,vol. 28, no. 6, pp. 29682979, Jun. 2013.

[11] J. H.Wohlgemuth and S. R.Kurtz,Howcan we make PV modules safer?,*in Proc. 38th IEEE Photovoltaic Spec. Conf.*,2012, pp. 31623165.

[12] W. Li and X. He,Review of nonisolated high-step-up dc/dc converters in photovoltaic grid-connected applications ,*IEEE Trans. Ind. Electron.*,vol. 58, no. 4, pp. 12391250, Apr. 2011.

[13] H.Wang and D. Zhang ,The stand-alone PV generation system with parallel battery charger ,*in Proc. IEEE ICECE*,Jun. 2010, pp. 44504453.

[14] M. J. V. Vazquez, J. M. A. Marquez, and F. S. Manzano ,A methodology for optimizing stand-alone PV-system size using parallel-connected dc/dc converters ,*IEEE Trans. Ind. Electron.*,vol. 55, no. 7, pp. 26642673,Jul. 2008.

[15] N. Mutoh and T. Inoue ,A control method to charge series-connected ultra electric double-layer capacitors suitable for photovoltaic generation systems combining MPPT control method ,*IEEE Trans.Ind. Electron*,vol. 54, no. 1, pp. 374383, Feb. 2007.

[16] R. Chattopadhyay and K. Chatterjee ,PV based stand alone single phase power generating unit ,*in Proc. IEEE IECON*,Oct. 2012, pp. 11381144.

[17] D. Debnath and K. Chatterjee,A buck-boost integrated full bridge inverter for solar photovoltaic based stand alone system ,*n Proc. IEEE PVSC*,Jun. 2013, pp. 28672872

[18] T.-F. Wu, C.-H. Chang, Z.-R. Liu, and T.-H. Yu, Single-stage converters for photovoltaic powered lighting systems with MPPT and charging features, *in Proc. IEEE APEC*, Feb. 1998, pp. 11491155.

[19] A. Testa, S. De Caro, T. Scimone, and S. Panarello, A buck-boost based dc/ac converter for residential PV applications, *in Proc. IEEE SPEEDAM*, 2012, pp. 114119.

[20] D. D.-C. Lu and V. G. Agelidis, Photovoltaic - battery-powered dc bus system for common portable electronic devices *IEEE Trans. Ind. Electron.*, vol. 24, no. 3, pp. 849855, Mar. 2009.

[21] D. Debnath and K. Chatterjee, Transformer coupled multi-input two stage stand alone solar photovoltaic scheme for rural areas, *in Proc. IEEE IECON*, Nov. 2013, pp. 70287033.